ISBN: 978-3-95450-202-8 doi:10.18429/JACoW-HB2018-TUP2WE01

INJECTION FOIL TEMPERATURE MEASUREMENTS AT THE SNS ACCELERATOR*

W. Blokland, N. Evans, C. Luck, A. Rakhman, Oak Ridge National Laboratory, Oak Ridge, USA.

Abstract

The SNS uses charge exchange injection to minimize losses during the accumulation of the accelerated beam in the ring. A stripper foil implements this by removing the electrons from the high intensity H- beam coming from the linac. At a beam power of 1.2 MW, the foil lasts for many weeks, sometimes months. However, given the upgrade to 2.8 MW, it is important to know the current temperature of stripper foil in order to estimate its lifetime for the new beam power and beam size. In this paper, we discuss several methods to measure the temperature of stripper foil exposed to current operating conditions of the SNS accelerator. Given the high radiation in the vicinity of the foil, the uncertainty in the foil's emissivity, and available resources, we chose a two-wavelength pyrometer that is located 40 m from the foil. The pyrometer is composed of two mirrors, a refracting telescope, and two photodiodes. We present the calibration data and the temporally resolved measurements made with this pyrometer.

INTRODUCTION

The Spallation Neutron Source (SNS) uses a nanocrystalline diamond foil, see Fig. 1, to implement a charge-exchange scheme to efficiently accumulate bunches from the linac into the ring to deliver a short and intense pulse to the target [1]. The lifetime of the foil is limited by temperature induced sublimation and by radiation damage [2]. Currently, the foils have lifetimes of several months, over 2500 MWHr of beam at 1.2 MW, before they need to be exchanged. Foils can be exchanged quickly with the foil exchanger, which has up to 12 foils installed. More beam power, such as planned for the Second Target Station, can lead to higher temperatures and these higher temperatures can reduce the lifetime of the foil, potentially complicating operations.

Figure 1: Unused foil, left, and used, right.

In the early days of SNS operations, when the foil lifetime was not yet known, attempts were made to measure temperatures in the tunnel with cameras. An unshielded infrared camera died immediately, even at the much lower beam powers at the time. A second attempt with a shielded visible light camera with two bandpass filters, a two-color pyrometer, was also not successful due to the radiation. However, we found by experience, that the foil lifetimes were high enough that we did not have to worry, and interest in measuring the foil temperature waned. However, with the eye on the future power upgrades, up to 2.8 MW, the interest in measuring the foil temperature and understanding the foil lifetime has been renewed.

OPTICAL PATH

Only two mirrors were needed to get light from the foil from the high radiation area to the Ring Service Building by using an existing and unoccupied cable chase. The disadvantage is the long path length, about 40 meters. This optical path was in use to look at the foil with a regular visible light digital camera mounted on a telescope, see Fig. 2. Figure 2 also shows, on the right, a picture made with a regular camera of the foil with the beam spot clearly visible.

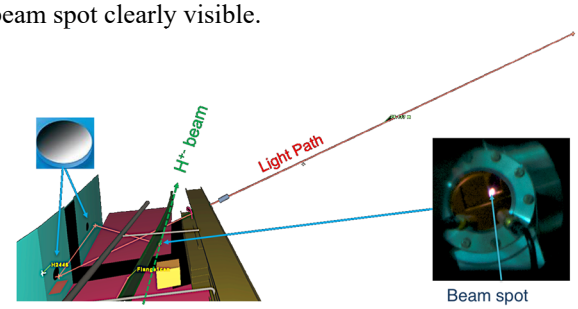

Figure 2: Optical light path to foil.

TWO-WAVE PYROMETER

A two-wave or two-color pyrometer removes the dependency of the temperature measurement on the emissivity by taking the ratio of the received light intensity from two different wavelengths. The pyrometer equation can be derived by dividing Planck's equation (1) for each wavelength's intensity and using Wien's approximation and assuming that the emissivity is the same for both wavelengths (2):

$$I(\lambda,\varepsilon,T) = \frac{2hc^2}{\lambda^5}\frac{\varepsilon(\lambda)}{e^{\frac{hc}{\lambda kT}}-1} \quad (1)$$

$$Ratio_{1/2} = \frac{s_1 I(\lambda_1,\varepsilon(\lambda_1),T)}{s_2 I(\lambda_2,\varepsilon(\lambda_2),T)} = \frac{s_1}{s_2}\left(\frac{\lambda_1}{\lambda_2}\right)^{-5} e^{\frac{2hc^2}{T}\left(\frac{1}{\lambda_2}-\frac{1}{\lambda_1}\right)} \quad (2)$$

The transmission coefficients, s_i, need to be determined through calibration for each wavelength. Ratio

*This manuscript has been authored by UT-Battelle, LLC, under Contract No. DE-AC05-00OR22725 with the U.S. Department of Energy. The United States Government retains, and the publisher, by accepting the article for publication, acknowledges that the United States Government retains a non-exclusive, paid-up, irrevocable, world-wide license to publish or reproduce the published form of this manuscript, or allow others to do so, for United States Government purposes. The Department of Energy will provide public access to these results of federally sponsored research in accordance with the DOE Public Access Plan (http://energy.gov/downloads/doe-public-access-plan).

ISBN: 978-3-95450-202-8 doi:10.18429/JACoW-HB2018-TUP2WE01

curves for different wavelength combinations are shown in Fig. 3. A combination of filters that gives a steeper curve, but still with enough radiance for the expected temperature, is often preferred to maximize the resolution.

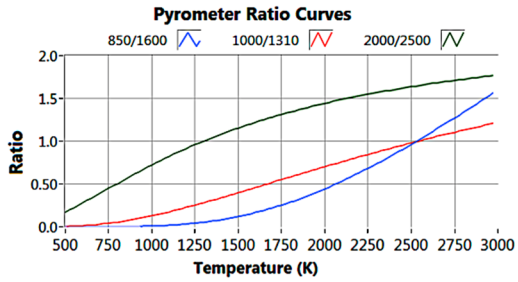

Figure 3: Different ratio curves for different filter combinations.

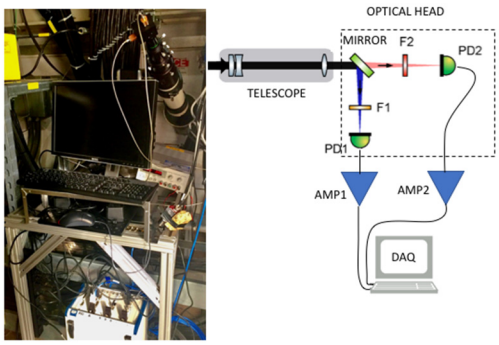

Figure 4: Pyrometer setup.

The implementation of our pyrometer is shown in Fig. 4. We manufactured an optical head with a dichroic mirror to reflect the shorter wavelengths to one photodiode and pass the longer wavelengths to a second photodiode. In front of each photodiode is an appropriate bandpass filter. The signals from the Hamamatsu G10899 InGaAs PIN photodiodes are amplified by the Femto DLPCA-200 current amplifiers and digitized by National Instruments PXI digitizers.

CALIBRATION

Optical Transmission and Reflections

To determine the transmission coefficients, s_i, we measured the spectral response of different optical elements, such as the vacuum window, glass window, telescope, dichroic mirrors, and bandpass filters. The photodiode has a detection range of approximately 0.4 to 1.7 µm. To measure over that range, we had to use two available optical spectrum analyzers, the Thorlabs CCS200, with a spectral range of 0.2 to 1.0 µm, and the Anritsu MS9740A, with a spectral range of 0.6-1.7 µm.

We found that several bandpass filters leak light outside their pass band. While a properly selected dichroic mirror can help reduce the leakage, one is better off with a bandpass filter that only lets through light in the pass band for the entire band of the photo detector. Figure 5 shows several of the measured bandpass filters. It shows that the 1050 nm filter leaks a lot of light above 1300 nm. If used with the right dichroic mirror, this bandpass filter could still be used. The long pass mirrors can also leak light outside their specifications, so combinations should be carefully selected. We selected bandpass filters with minimal leakage.

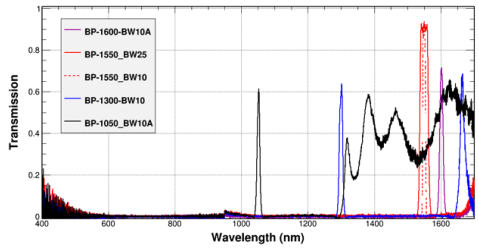

Figure 5: Bandpass measurements.

While it was relatively easy to measure the transmission of the mirrors, windows, and bandpass filters with the optical spectrum analyzers, it was very difficult to measure the telescope transmission given the fiber-coupling requirement. Also, because of the large difference in transmission for the visible light and the near infrared light, we are not sure how accurate the offset on this measured curve is, thus enabling a potentially large error in a s_i for the near infrared range.

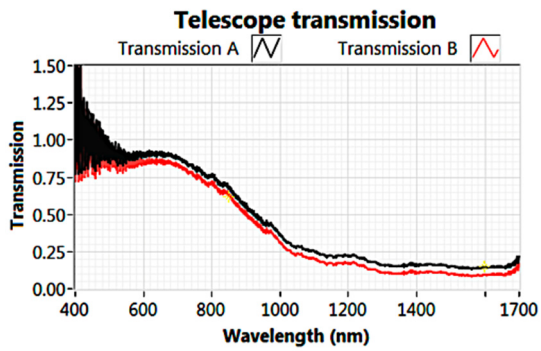

Figure 6: Telescope transmission measurement.

For example, see Fig. 6, looking at just moving the curve, transmission A, down by 0.05 to get transmission B, changes the 800 nm transmission from 0.67 to 0.62, but the 1600 nm transmission changes from about 0.15 to 0.1 leading to an almost 50% change. This can lead to a temperature error of about 125 K, if the temperature is 1500 K. We hope to redo this measurement once the new free space optical spectrometer has been delivered.

Blackbody Source

Beginning of April of this year, we had the availability of a blackbody source, the LumaSense M305. We used this source to calibrate two optical heads, one with 850 and 1600 nm bandpass filters and a 1000 nm longpass dichroic mirror, and one with a 1000 and 1310 nm bandpass as well as an 1180 nm longpass dichroic mirror.

The setup is shown in Fig 7. We used the same mirrors as installed in the tunnel to fold the optical path in the lab for an approximate 20 meters path length. We measured the response up to 1273 K, the maximum of the black-

ISBN: 978-3-95450-202-8 doi:10.18429/JACoW-HB2018-TUP2WE01

body source. The measured ratios for the 1000/1310 head are shown in Table 1. We calibrated by applying a single multiplier, 0.89, to the ratios to match the blackbody temperature with the calculated temperature. We can now use this same multiplier in the field with the foil to derive the foil peak temperature, instead of using the optical transmission measurements. We also calibrated the 850/1600 optical head with the blackbody source and also got well within 1% and with steps close to 100 K. However, there was a significant difference, 1.8 times, with the optical transmission calculated multiplier. Given the uncertainty in the telescope calibration, we will use the blackbody source derived multiplier for the foil temperature measurements.

Figure 7: Using the blackbody source for calibration.

Table 1: Optical Head 1000/1310 Calibration

BB T (K)	Measured Ratio	New Ratio (x0.89)	Calculated T (K)	Error %
1073.2	0.181	0.162	1073.1	-0.02
1173.2	0.238	0.213	1175.1	0.21
1273.2	0.298	0.267	1273.1	0.09

BEAM SPOT

The telescope is mounted on a motorized mount and our initial plan was to put a pinhole in front of the photodiodes and scan the telescope across the foil to build up an image. However, the pinhole had to be as big as the projected beam spot to get enough signal-to-noise. To be able to estimate the peak temperature from the whole beam spot, we assumed that the gaussian beam from the linac produces the same gaussian temperature distribution. We also assumed that the emissivity is constant over the beam spot and that we projected the complete beam spot on each photodiode. The new radiation curve then becomes a summation of many blackbody radiators, see (3).

$$BBS(T) = \sum_{\substack{-l<x<l \\ -k<y<k}} BB\big(T(x,y)\big) \qquad (3)$$

The change in the radiation spectrum is shown in Fig 8. The curve named BB is the standard blackbody radiation curve and the BBS (BlackBody Sum) curve is the sum of a gaussian temperature distribution. The BBA (BlackBody Accelerator physics) curve represents the calculated beam spot [3], shown on the right side of the figure. The BBA includes the hits from protons circulating in the ring. The difference between the BBS and BBA curves is very small and leads to small differences in the calculated temperatures of about 5 to 10 K.

We verified that the projected beam spot is much smaller than the photodiode sensitive area by using a camera image to calculate the projected spot size from the pixel size and pixels occupied by the image. The visible light part of the projected spot is around 200 µm, much smaller than the 3 mm photodiode area. The telescope aim is adjusted until both photodiodes reach their maximum signal for the conditions.

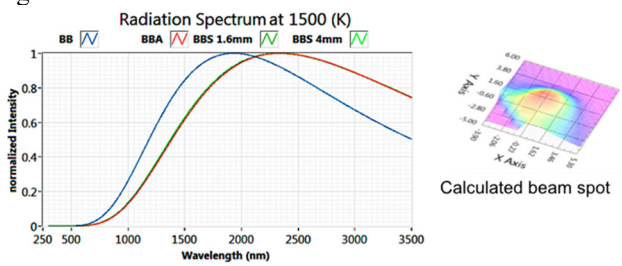

Figure 8: Radiation Spectra.

MEASUREMENTS

Signals

A typical signal measured from the photodiodes is shown in Fig 9. Every 16.6 ms, an approximately 1 ms long pulse hits the foil. We see a steep rise in the signals followed by a much longer decay. The signals are filtered with a median and/or a Savitzky-Golay filter to reduce the noise.

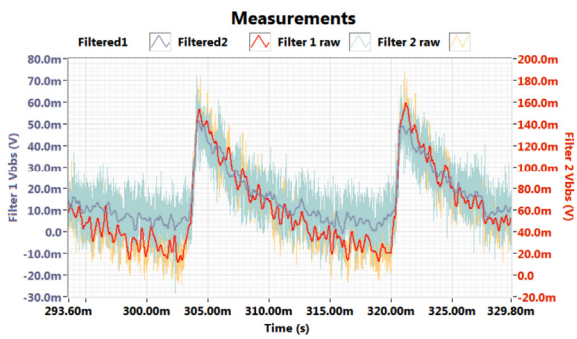

Figure 9: Raw and filtered photodiode signals.

The filtering still leaves too much noise to take the ratio of the signals. To further reduce the noise, we apply a rather stiff spline fit to smoothly follow the steep rise and the decay. To allow for the spline to quickly change direc-

ISBN: 978-3-95450-202-8 doi:10.18429/JACoW-HB2018-TUP2WE01

tion from the cooling curve to the heating slope and vice versa, the spline is relaxed around those turning points, see Fig 10.

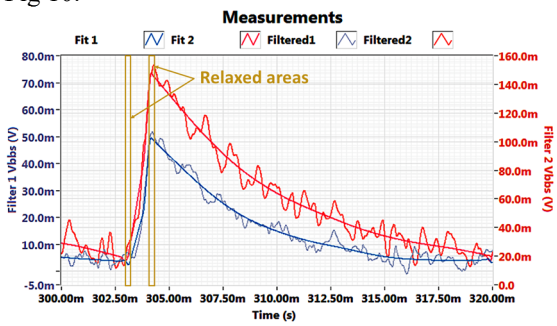

Figure 10: The filtered and fitted photodiode signals.

Studies

To test the prototype pyrometer, we set the linac up to deliver exactly 20 beam pulses, each 1ms long. This allows us to see the baseline, the heating up of the foil, and the full cool down curve after the last pulse, see Fig 11. The first pulse is barely or not visible as the temperature still has to build up with the following pulses.

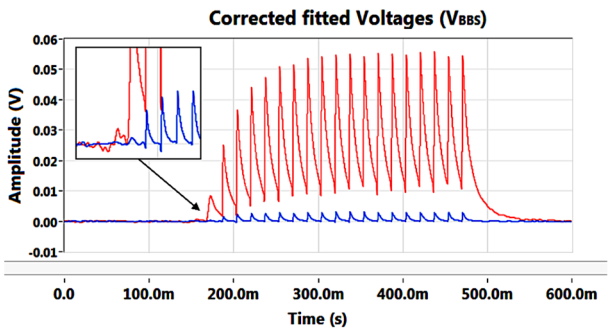

Figure 11: The signals for 20 pulses.

Data from 1.3 MW equivalent pulses are shown in Fig. 12 for the 850/1600 optical head and in Fig. 13 for the 1000/1310 optical head. Both measurements show a temperature between 1450 and 1500 K. The same foil was running at about 1600 K earlier in the run.

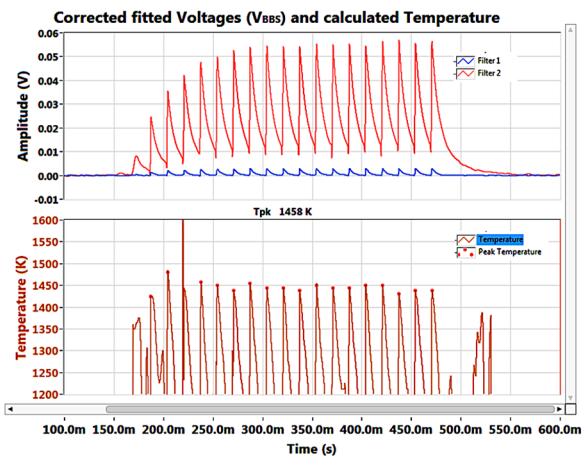

Figure 12: Calculated temperature curves using the 850/1600 optical head.

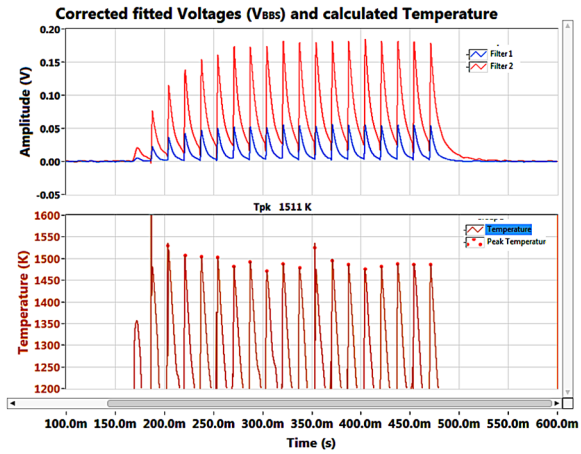

Figure 13: Calculated temperature curves using the 1000/1310 optical head.

Control Room Screen

The data from the pyrometer is available over EPICS in the control room so we can observe the temperature over time and archive the data. The Control Room screen is shown in Fig. 14. At this point the foil is being conditioned and its peak temperature is 1700 K.

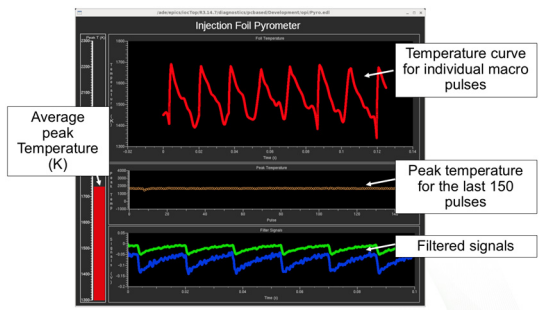

Figure 14: EDM screen during conditioning.

Foil Conditioning

We condition a foil before using it in a production run to extend its life. Foil conditioning consists of running beam at lower power and over approximately half a day, slowly increasing the beam power up to full production levels. From experience we know that if a foil is not conditioned, it does not last long. The Raman spectra of the conditioned foils show strong peaks from graphitic carbon which has a higher emissivity of around 0.8 instead of about 0.4 for diamond, see [4].

The overall conditioning process is shown in Fig 15. The temperature of the new foil, the red trace, starts out at above 2000 K. We see the vacuum pressure, the green trace, go up as the foil is conditioning. But the temperature goes down quickly, as well as the vacuum pressure. The beam power, the blue trace, is then increased, and we see that the temperature increases again and the vacuum pressure going up. However, soon after each beam power increase, the temperature eventually decreases, and the vacuum pressure goes down. The foil temperature stabilizes to around 1700 K during the conditioning process.

ISBN: 978-3-95450-202-8 doi:10.18429/JACoW-HB2018-TUP2WE01

Over time, the foil will go down even further to 1600 K or less.

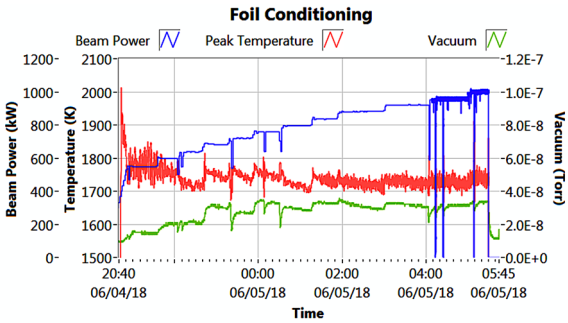

Figure 15: Foil conditioning.

Foil Sublimation

The foil sublimation due to high temperatures is a main factor of the foil lifetime. We defined the lifetime of the foil to end once 30% of the foil has sublimated. Radiation damage is another factor but not considered in this paper. An equation for foil sublimation can be found in [2]:

$$\frac{dh(t)}{dt} \cdot \frac{1}{\rho} = -4.06 \cdot 10^{8} \cdot \frac{e^{\left(-\frac{83500}{T}\right)}}{\sqrt{T}} \qquad (4)$$

The density of the foil, ρ, is approximately 3.5 g/cm^3 for diamond and about 2.2 g/cm^3 for graphite. We used this equation and the density for graphite to calculate the foil sublimation as a function of the temperature. At the lower temperatures of the foil, 1500 K, there is no limitation to the foil lifetime due to sublimation as this is integrated to be around $5.4 \cdot 10^{-14}$ m per day, see Fig. 16. At a temperature of around 2100 K, the foil loss would be about $8.5 \cdot 10^{-8}$ m per day which would give a lifetime estimated of only a few days with the pulsed SNS beam.

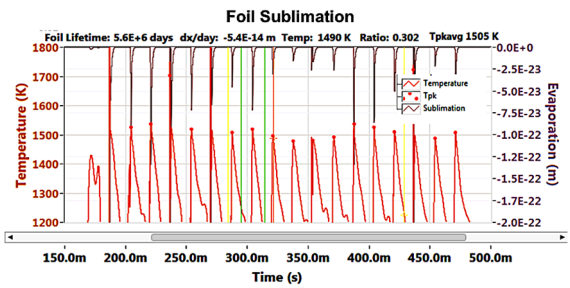

Figure 16: Sublimation of the foil along the temperature per pulse.

Radiative Cooling

We have started looking at the cooling curve of the foil, assuming there is only radiative cooling and assuming the foil temperature is much higher than the environment temperature, the expected temperature is:

$$T = T_{pk} \Big/ \sqrt[3]{1 + 3kT_{pk}^{3} \cdot t} \quad \text{with } k = \frac{2\varepsilon\sigma A}{3Nk_B}$$

$$\text{with } \sigma = 2\pi^5 k^4 / 15h^3 c^2 = 5.76\ 10^{-8}\ \mathrm{W/m^2K^4}$$

This means that we need to know the foil's thickness and emissivity. We know that the foil has a different thickness and/or density after conditioning, but we don't know this number given that the foil turns graphite-like and the possible sublimation or outgassing during foil conditioning process. While we have developed code to fit the measured cool down curve, again assuming that our signal is derived from the 2-D sum of gaussians, the wide range in parameters means that a wide range, > 150 K, in temperature is possible. We hope to look closer at this technique in the near future. An example of the analysis is shown in Fig 17. The graph on the left shows the cooldown curve of the last pulse with fit, while on the right side the pulse train is shown. With best estimates for emissivity, 0.83 and assuming 1 µm thickness of graphite, a reasonable temperature can be calculated, 1628 K, as shown in Fig. 17.

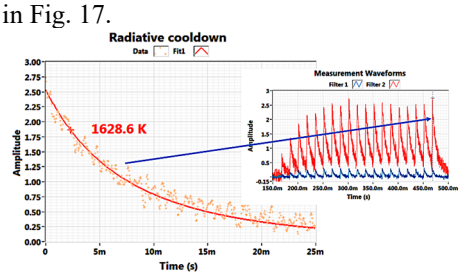

Figure 17: Estimation of the foil peak temperature based on the cooldown curve.

DISCUSSION AND FUTURE

We have installed a new prototype foil temperature measurement system and can now start correlating the foil temperature with actual foil lifetime, accelerator setup, and variations in beam parameters. Already, we have been able to use it to observe the foil conditioning process. The temperature is estimated around 1500-1600 K at 1.3 MW beam power. We are still looking at the errors due to the assumptions, but estimate that the errors due to signal noise, signal processing, and fitting are less than ± 100 K. Further improvements in the code can be made to reduce these errors.

Further increases in signal-to-noise can be made by a combination of widening the bandpass filters, using more sensitive, possibly cooled detectors, and optics in the tunnel to increase light collection. Much better light collection will also allow the use of cameras with bandpass filters in front to create a 2-D temperature picture of the beam spot, eliminating the need for assuming a gaussian distribution.

Developments in the foil testing in the lab will help with further establishing the foil's emissivity and the foil sublimation process. The foil lab's measurements, coupled with the field temperature measurements, will provide estimates for foil lifetimes at higher temperatures, and should help us improve the analysis of the cooldown curve, increasing our confidence in the measured temperature.

We also plan to compare the infrared camera measurements with the pyrometer measurements in the foil lab.

ISBN: 978-3-95450-202-8 doi:10.18429/JACoW-HB2018-TUP2WE01

REFERENCES

[1] J. Wei, *et al.*, "Low-Loss Design for the High- Intensity Accumulator Ring of the Spallation Neutron Source," *Phy. Rev. Lett. ST Accel. Beams*, vol. 3, p. 080101, Aug. 2000, doi:10.1103/PhysRevSTAB.3.080101

[2] Lebedev S.G. *et al.*, "Calculation of the lifetimes of thin stripper targets under bombardment of intense pulsed ions," *Phy. Rev. Lett. ST Accel. Beams*, vol. 11, p. 020401, Feb. 2008, doi:10.1103/PhysRevSTAB.11.020401

[3] Plum M., *et al.*, "SNS stripper foil development program," *Nucl. Instr. Meth*, vol. 590, Iss. 1–3, pp. 43-46, 2008, doi:10.1016/j.nima.2008.02.065

[4] Barrowclough E.P., "Analysis of Primary Stripper Foils at the Spallation Neutron Source by an Electron Beam Foil Test Stand," Ph.D. thesis, Chem. Dept., University of Tennessee, Knoxville, USA.